Available online at www.sciencedirect.com

SciVerse ScienceDirect

Journal of Magnesium and Alloys 1 (2013) 64–75
www.elsevier.com/journals/journal-of-magnesium-and-alloys/2213-9567

Full length article

Microstructure evolution of extruded Mg-Gd-Y magnesium alloy under dynamic compression

Mao Ping-li*, Yu Jin-cheng, Liu Zheng, Dong Yang

School of Materials Science and Engineering, Shenyang University of Technology, Shenyang 110870, China

Abstract

For the purpose of investigating the microstructure evolution and deformation behavior of magnesium under high strain rates, the Split Hopkinson Pressure Bar (SHPB) apparatus was used under high strain rates from 755 s^{-1} to 2826 s^{-1} in the present work at room temperature. The microstructures of extruded Mg-Gd-Y Magnesium alloy under different strain rates and along different compression directions were observed by metallographic microscope. The results show that, microstructures of extruded Mg-Gd-Y Magnesium alloy along ED, TD and ND compression directions are sensitive to strain rates. The amount of twins firstly increases and then decreases with strain rates being increased, and the recrystal grains increase and grow up. When the strain rate reaches 2500 s^{-1}, the adiabatic shear band (ASB) begins to form. The formation process of the adiabatic shear band can be divided into three stages. In the first stage, under the impact load a great deal of twins form and the deformation mechanism is twinning. In the second stage, discontinuous ASB forms due to twins adjusting the directions of located grains and the deformation mechanisms are twinning and non-basal slip. In the last stage, non-basal slip turns to basal slip and continuous ASB forms. The dynamic compression fracture mechanism of extruded Mg-Gd-Y Magnesium alloy is multi-crack propagation.

Keywords: Magnesium alloy; SHPB; Microstructure evolution; ASB; Deformation mechanism

1. Introduction

Magnesium alloys are the lowest density of the metal structure material which have been widely applied to the automotive field due to the advantages of high specific strength, high specific stiffness, good damping capacity and machinability [1,2]. Conventional magnesium alloys have poor heat resistance and high temperature creep resistance and usually only used under 120 °C. However it is a restriction of conventional magnesium alloys because the transport engine and transmission components require the materials withstanding temperatures of more than 250 °C. Thus large numbers of studies have been conducted to add rare-earth into magnesium alloys to improve the mechanical property, corrosion-resistance, high temperature performance and creep resistance of cast magnesium alloys and spectacular results have been achieved [3]. In recent years magnesium alloys used at the temperature above 200 °C are all magnesium rare-earth alloy. On the basis of Mg-Gd alloys, Mg-Gd-Y(-Zr/Mn) alloy system added a certain Y, Zr(or Mn) has become one of the high strength cast and wrought magnesium systems [4]. Automobile component is the one of the main application of magnesium alloys and the adequate application performance of magnesium alloys and their components need to be provided to match the application. In most studies of magnesium rare-earth attention has been given to erosion resistance and heat resistance. There have been little amount of studies highlight the dynamic mechanical property of magnesium rare-earth alloys and it is a

* Corresponding author. Tel./fax: +86 024 25497131.
E-mail address: pinglimao@yahoo.com (M. Ping-li).
Peer review under responsibility of National Engineering Research Center for Magnesium Alloys of China, Chongqing University

http://dx.doi.org/10.1016/j.jma.2013.02.007

Table 1
Chemical compositions of extruded Mg-Gd-Y alloy (mass fraction, %).

Mg	Gd	Y
87.22	08.05	04.74

limitation to use magnesium rare-earth alloys complying with the actual usage. Ji Wei and Fan Ya-fu [5] found that after dynamic tension under strain rate of 10^3 s^{-1} and at the temperature of 150–525 °C the failure mechanism of two types of extruded Mg-Gd-Y alloys were shallow dimple and mixed quasi-cleavage fracture. $T \leq 400$ °C, the failure mechanism turned into an inter-granular fracture due to grain boundary softening with increased temperature. Moreover the main deformation mechanism was basal slip and non-basal slip system would fully start with the temperature being increased. Also the percentage of elongation reached a maximum when the temperature reached 450 °C.

In the author's laboratory, Split Hopkinson Pressure Bar (SHPB) was used for investigating dynamic mechanical properties of extruded Mg-Gd-Y Magnesium alloy at room temperature. We found that extruded Mg-Gd-Y Magnesium alloy under dynamic compression along ED, TD and ND directions yielded continuously, and had the positive strain rate effect when strain rates increasing. Dynamic mechanical properties did not exhibit strong anisotropy and along ED direction were relatively optimal. The fracture performance of extruded Mg-Gd-Y Magnesium alloy along different directions was mix-fractured quasi-cleavage fracture and was not sensitive to the loading direction. The deformation mechanism of extruded Mg-Gd-Y Magnesium alloy under high stain rate compression was a combination of twinning, slipping and dynamic recrystallization. However there are still a few problems existing in the study on the dynamic mechanical property of magnesium alloys, for example there are not any experiment or research on the microstructure evolution after deformation, micro-mechanism of dynamic deformation and micro-mechanism of crack formation, crack propogation and failure breaking [6]. The present study of metal's microstructure evolution mainly focus on [7]: (1) dislocation glide, increase of dislocation density and formation of dislocation substructure; (2) changes of micro-crystallography orientation and formation of micro-texture; (3) evolution of dislocation cells, dislocation interface spacing, subgrain and grain size; (4) changes of dislocation interface, sub-boundary and grain boundary character; (5) changes in the statistical of crystal orientation, namely formation of marcotexture. In addition there are few reports on characteristics of the microstructure and its evolution of interior region of deformation localization (such as shear band) when large strain, cold-deformed metal under high strain rate compression [8]. Ji Wei [9] observed that the adiabatic shear band (ASB) was a white band in magnesium alloy (Mg-Gd-Y system) target but he did not investigate the microstructure evolution of ASB. Thus in this work we report in detail the microstructure evolution within ASB of extruded Mg-Gd-Y magnesium alloy under high strain rate and analyze its deformation behavior and fracture mechanism. The micro-structural characterization of deformed specimens was performed using light optical microscopy (LOM).

2. Material and specimens

The extruded Mg-Gd-Y magnesium alloy was provided by Beijing General Research Institute for Non-ferrous Metals, whose chemical compositions are listed in Table 1. The samples of dynamic compression were cut from the Mg-Gd-Y magnesium extrusion (Fig. 1(a)) along different directions as shown in Fig. 1(b) and the size is φ8 × 6 mm.

3. Results

3.1. Dynamic compressive properties

The Split Hopkinson Pressure Bar (SHPB) was used under different strain rates at ambient temperature. The experiment device and methods can be found in papers [10–12]. The strain rates in SHPB experiments ranged from 755 s^{-1} to 2826 s^{-1}. The dynamic compressive true stress-true strain curves of extruded Mg-Gd-Y magnesium alloy at room temperature are shown in Fig. 2. Dynamic mechanical properties along ED, TD and ND direction are not anisotropy. Relatively along ED direction the strain rate is the maximum when the sample cracks and the fracture strength and fracture strain along ED direction are the maximum respectively, which implies the dynamic compressive property of extruded

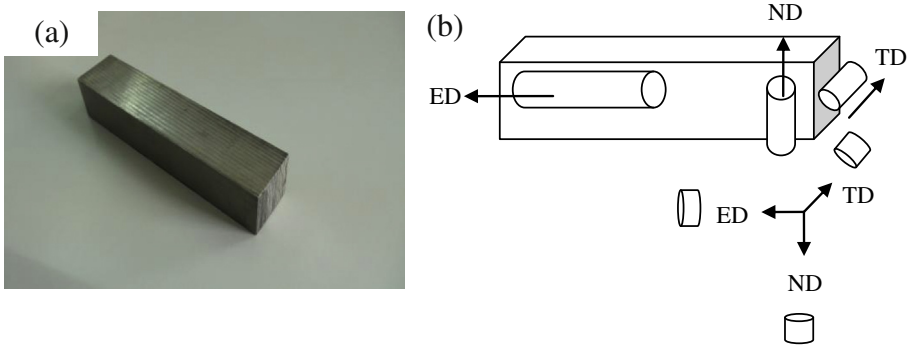

Fig. 1. (a) Photograph of extruded section; (b) extrusion direction of samples.

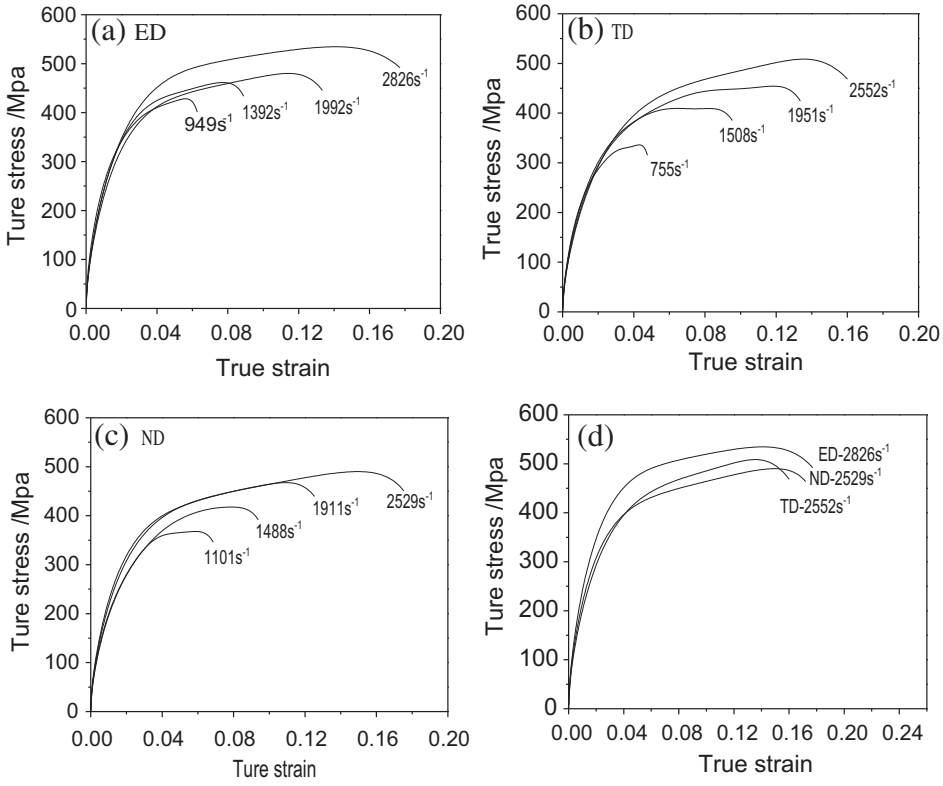

Fig. 2. Dynamic compressive true stress-true strain curves of Mg-Gd-Y magnesium alloy: (a) ED; (b) TD; (c) ND; (d) comparison of three directions.

Mg-Gd-Y magnesium alloy along ED direction is relatively the best among three directions.

The specimens after dynamic compression (as shown in Fig. 3) were made into metallographic samples. When the strain rate reached 2826 s^{-1} under ED compression, the sample cracked. When the strain rate reached 2552 s^{-1} under TD compression, the sample cracked. When the strain rate reached 2529 s^{-1} under ND compression, the sample cracked. Along three directions, the microstructures of section perpendicular to loading direction and microstructures of section parallel with the loading direction were observed in unbroken specimens. Along three directions, the microstructures of section perpendicular to loading direction, the microstructures of section parallel with loading direction and microstructure of the diagonal section were observed in broken specimens.

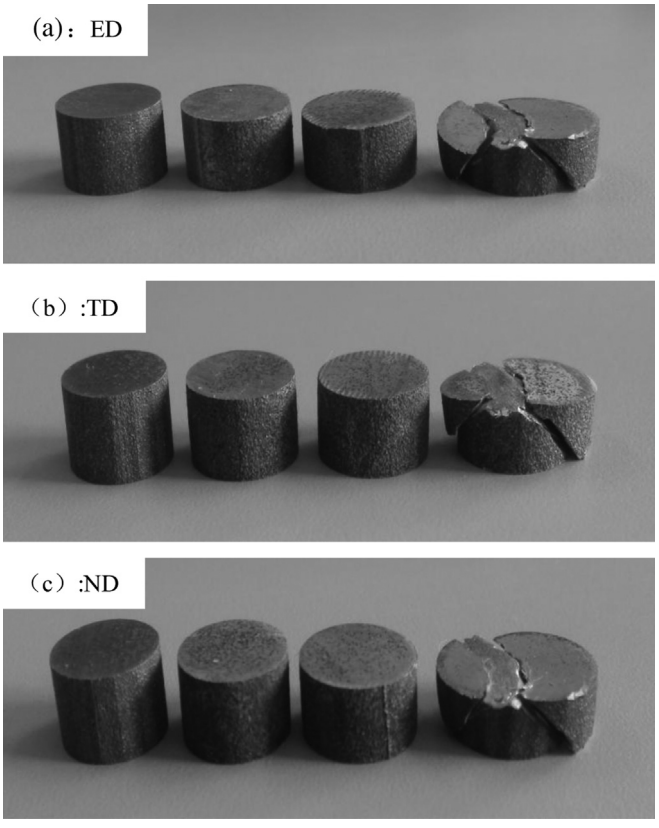

Fig. 3. (a) Photograph of samples after dynamic compression: (a) ED direction; (b) TD direction; (c) ND direction.

3.2. Dynamic microstructure evolution

3.2.1. Micro-structural characterization along ED direction

Fig. 4 shows the microstructures of section perpendicular to the loading direction along ED direction. As shown in Fig. 4(a), original microstructure of extruded Mg-Gd-Y magnesium alloy along ED direction is a typical extrusion state microstructure. There is a great amount of uniform equiaxed big-sized grains whose size are about 10 μm and a few of small sized recrystallization grains which lie between the big-sized grains and can be seen in the black striped area in Fig. 4(a). In addition no twins are in both of the big and small sized grains. Fig. 4(b)−(e) are the microstructures of section perpendicular to loading

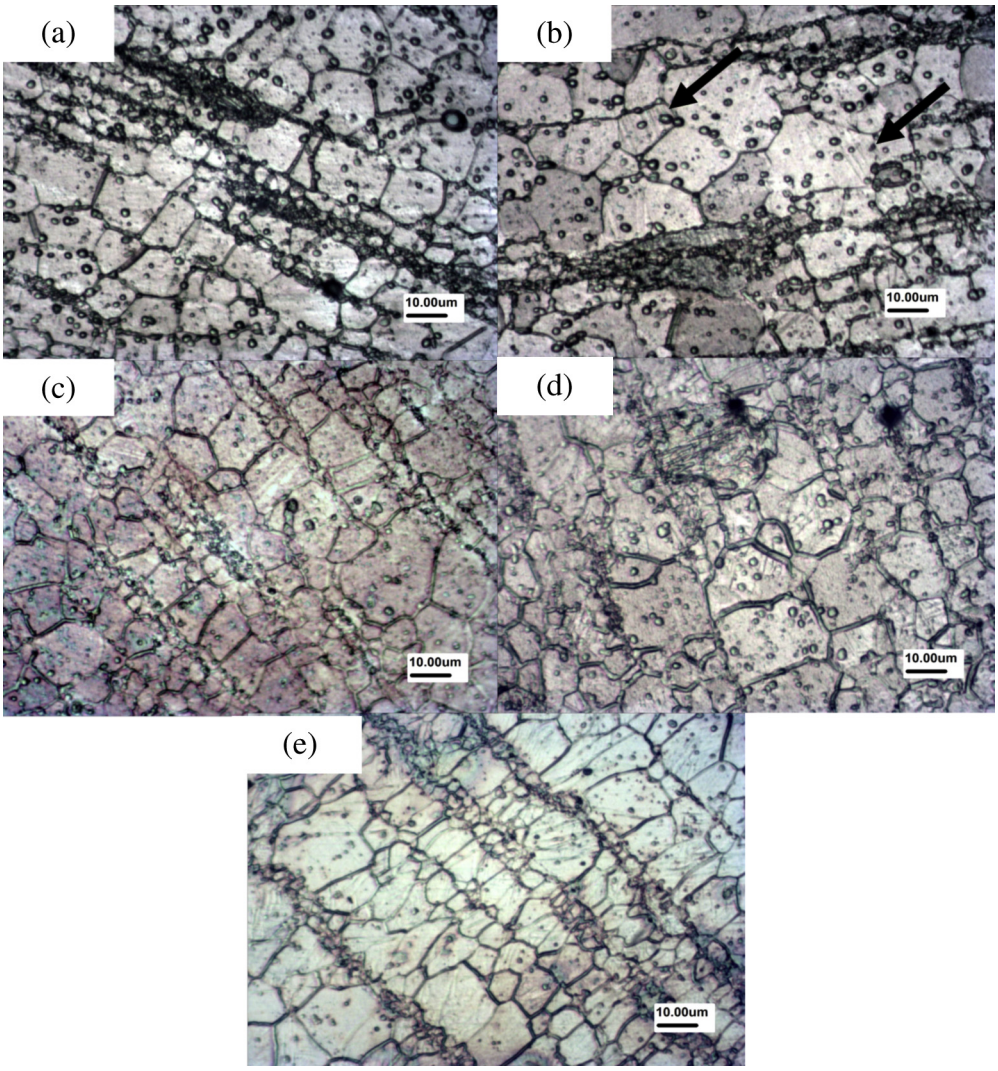

Fig. 4. Microstructures of section perpendicular to loading direction along ED direction: (a) original microstructure; (b) under strain rate of 949 s^{-1}; (c) under strain rate of 1392 s^{-1}; (d) under strain rate of 1992 s^{-1}; (e) under strain rate of 2826 s^{-1}.

direction along the ED direction under strain rates of 949 s^{-1}, 1392 s^{-1}, 1992 s^{-1} and 2826 s^{-1} respectively. The results show that twinning happens in only several grains which are both big-sized grains and small sized grains, as shown in Fig. 4(b). The amount of twins increases and then decreases with strain rates being increased. Moreover, original recrystallized grains become more and coarsening and the recrystallization bands become wide and continuous in a row.

Fig. 5(a)–(e) are the microstructures of section parallel with loading direction along the ED direction under strain rates of 949 s^{-1}, 1392 s^{-1}, 1992 s^{-1}, 2826 s^{-1} and 2826 s^{-1} respectively. The results show that twinning happens in only several grains and the amount of twins increases and then decreases with strain rates being increased. Under the strain rate of 1392 s^{-1}, the amount of the twin is the maximum, as shown in Fig. 5(b). When the strain rate reaches 1992 s^{-1}, the uncontinuous white band appears along the recrystal grains, as shown in Fig. 5(c)–(e), under the strain rate of 2826 s^{-1}, the continuous white band appears and its average width is 3 μm. The white band is parallel with the band of recrystallized grains and separates equiaxed grains from recrystallized grains. Original recrystallized grains become more and coarsening and the recrystallization bands become wide and continuous with increased strain rates.

Fig. 6 shows the microstructure of the diagonal section after compression along ED direction. There are many paralleled cracks in the broken specimen as shown in Fig. 6(a) and (b). It indicates that the dynamic failure mechanism of magnesium is muti-crack propagation and cracks propogation along the grain boundary, as shown in Fig. 6(c). Similarly, twinning happens in only several grains in diagonal section.

3.2.2. Micro-structural characterization along TD direction

Fig. 7 shows the microstructures of section perpendicular to the loading direction along TD direction. Fig. 7(a) shows the original microstructure of extruded Mg-Gd-Y magnesium alloy along TD direction. There are a great amount of uniform equiaxed big-sized grains whose size are about 10 μm and a small amount of small sized recrystallization grains which lie between the big-sized grains. And no twins are in both of the

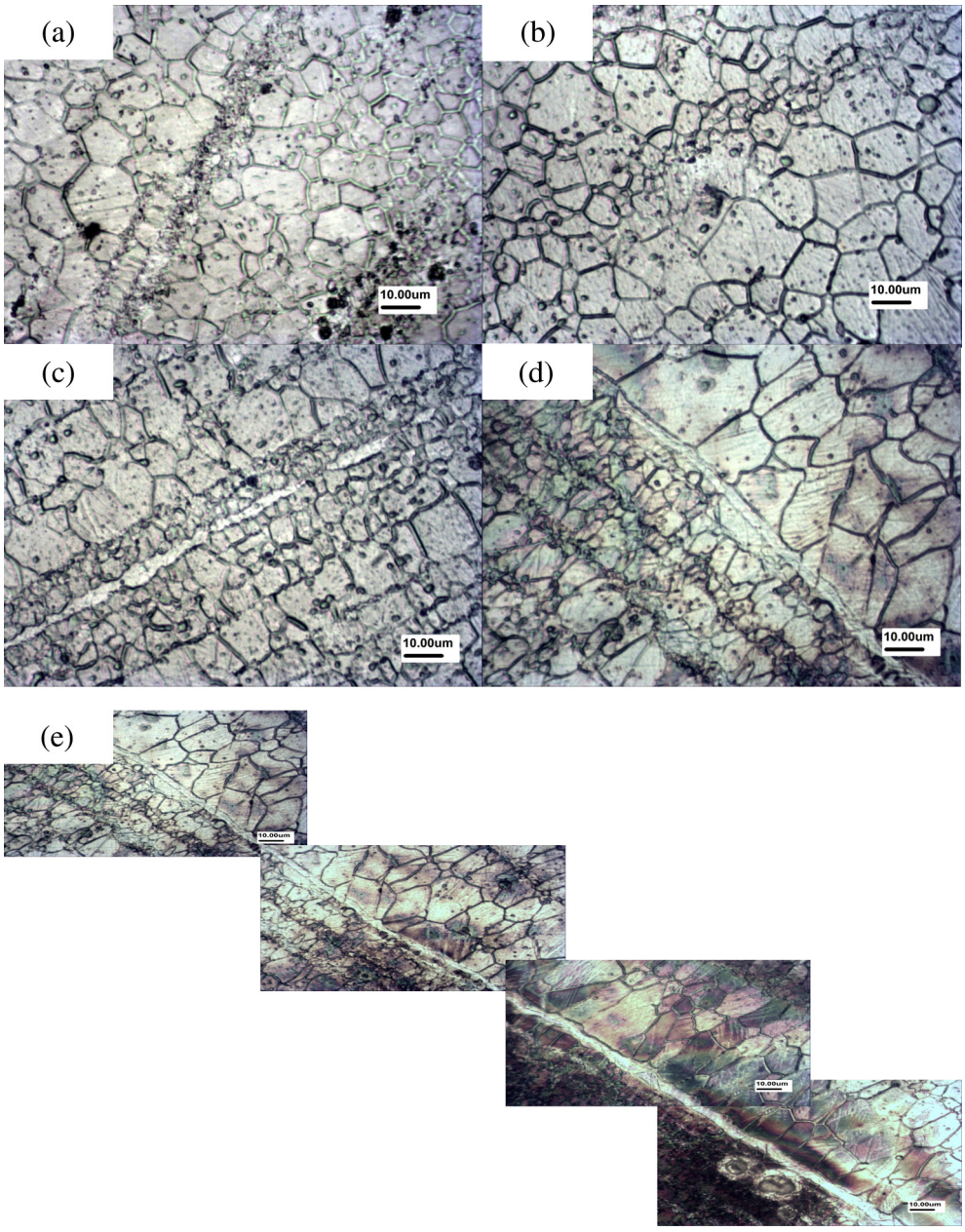

Fig. 5. Microstructures of section parallel with loading direction along ED direction: (a) under strain rate of 949 s^{-1}; (b) under strain rate of 1392 s^{-1}; (c) under strain rate of 1992 s^{-1}; (d) under strain rate of 2826 s^{-1}; (e) under strain rate of 2826 s^{-1}.

big and small sized grains. Fig. 7(b)–(e) are the microstructures of section perpendicular to loading direction along the TD direction under strain rates of 755 s^{-1}, 1508 s^{-1}, 1951 s^{-1} and 2552 s^{-1} respectively. The results show that twinning happens in only several grains which are both big-sized grains and small sized grains, as shown in Fig. 7(b). The amount of twins increases and then decreases with strain rates being increased. When the strain rate reaches 1508 s^{-1}, the uncontinuous white band appears along the recrystal grains, as shown in Fig. 7(c). Under the strain rate of 1951 s^{-1}, the white band is also uncontinuous, as shown in Fig. 7(d). Fig. 7(e) shows that, under the strain rate of 2552 s^{-1}, the continuous white band appears and its average width is 4 μm. The white band is parallel with the band of recrystal grains and twin band can be observed in the white band (shown in Fig. 7(d) and (e)). Original recrystallized grains become more and coarsening and the recrystallization bands become wide and continuous with increased strain rates, as shown in Fig. 7(c).

Fig. 8(a)–(f) are the microstructures of section parallel with loading direction along the TD direction under strain rates of 755 s^{-1}, 1508 s^{-1}, 1951 s^{-1} and 2552 s^{-1} respectively. The results show that twinning happens in only several grains and the amount of twins increases and then decreases with strain rates being increased. Under the strain rate of 1951 s^{-1}, the amount of the twins is the maximum, as shown in Fig. 8(e). Under the strain rate of 1508 s^{-1}, the abnormal big grain is observed and there are amount of twins in it, as shown in Fig. 8(c) and (d).

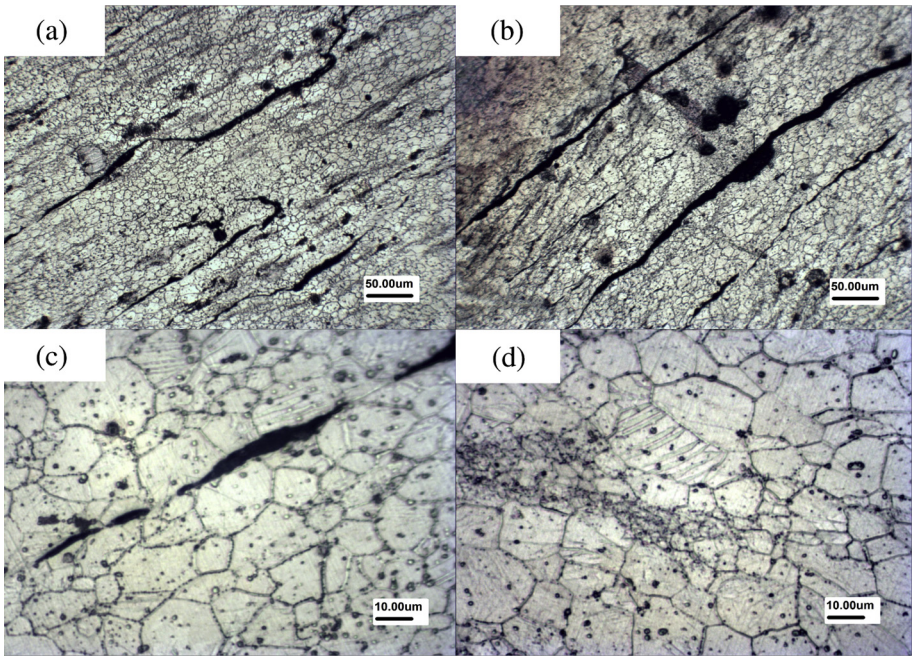

Fig. 6. Microstructure of the diagonal section after compression along the ED direction under strain rate of 2826 s^{-1}.

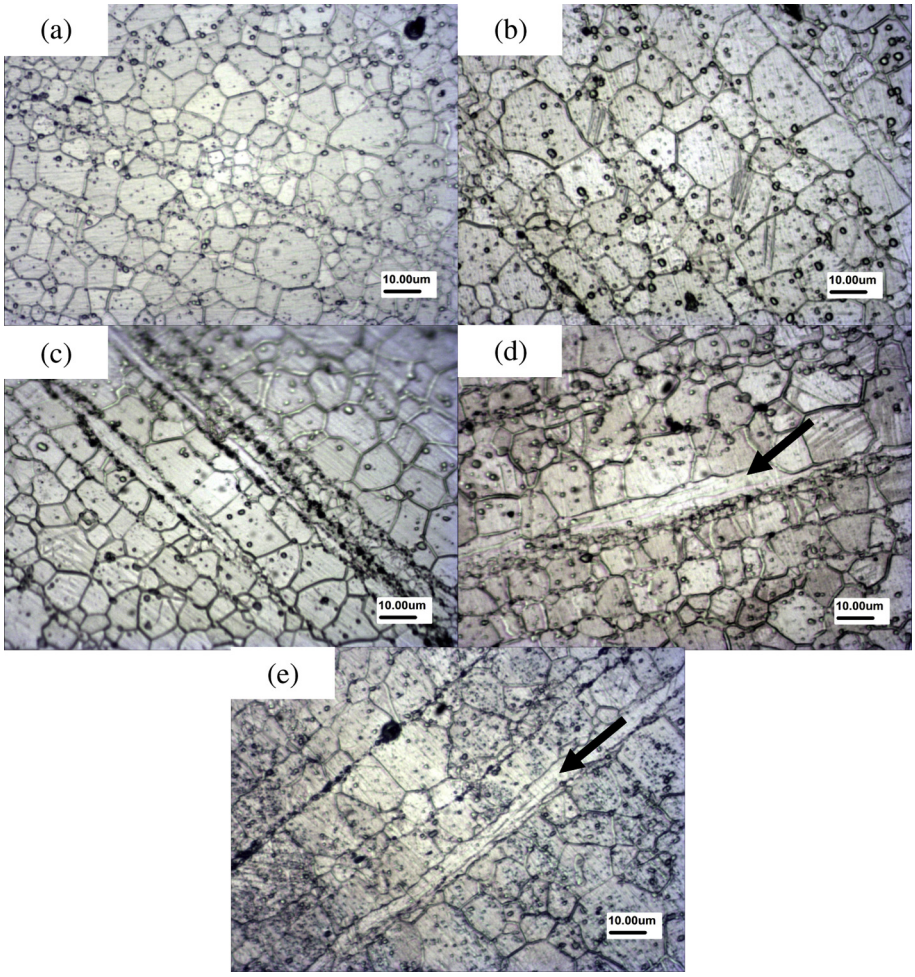

Fig. 7. Microstructures of section perpendicular to loading direction along TD direction: (a) original microstructure; (b) under strain rate of 755 s^{-1}; (c) under strain rate of 1508 s^{-1}; (d) under strain rate of 1951 s^{-1}; (e) under strain rate of 2552 s^{-1}.

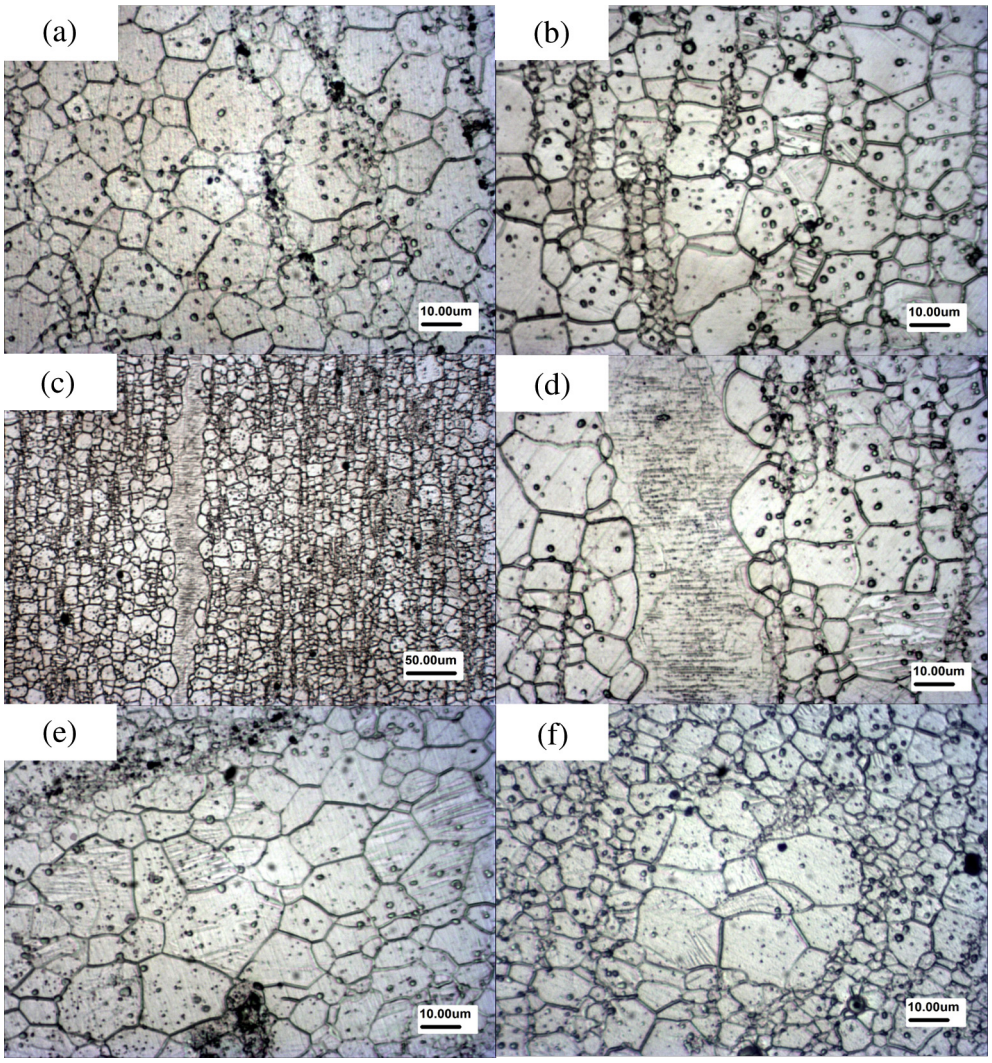

Fig. 8. Microstructures of section parallel with loading direction along TD direction: (a) under strain rate of 755 s^{-1}; (b) under strain rate of 1508 s^{-1}; (c) under strain rate of 1508 s^{-1}; (d) under strain rate of 1508 s^{-1}; (e) under strain rate of 1951 s^{-1}; (f) under strain rate of 2552 s^{-1}.

Fig. 9 shows the microstructure of the diagonal section after compression along TD direction. Under the strain rate of 2552 s^{-1}, the continuous white band appears and its average width is 2 μm.

3.2.3. Micro-structural characterization along ND direction

Fig. 10 shows the microstructures of section perpendicular to the loading direction along ND direction. As shown in Fig. 10(a), original microstructure of extruded Mg-Gd-Y magnesium alloy along ND direction is divided into equiaxed big-sized grains and small sized recrystallization grains. No twins are in both of the big and small sized grains. Fig. 10(b)−(e) are the microstructures of section perpendicular to loading direction along the ND direction under strain rates of 1101 s^{-1}, 1488 s^{-1}, 1911 s^{-1} and 2529 s^{-1} respectively. The results show that twinning happens in only several grains which are both big-sized grains and small sized grains, as shown in Fig. 7(b). The amount of twins increases and then decreases with strain rates being increased. Under the strain rate of 1488 s^{-1}, the amount of the twins is the maximum.

Fig. 11(a)−(d) are the microstructures of section parallel with loading direction along the ND direction under strain rates of 1101 s^{-1}, 1488 s^{-1}, 1911 s^{-1} and 2529 s^{-1} respectively. The results show that, when the strain rate reaches 1101 s^{-1}, the uncontinuous white band appears. There is no continuous white band with increased strains rate. Original recrystallized grains become more and coarsening. Twinning happens in only several grains. The amount of twins increases and then decreases with strain rates being increased. When the strain rate reaches 1488 s^{-1}, the amount of the twins is the maximum, as shown in Fig. 11(b). Under the strain rate of 2529 s^{-1}, the cracks propogate along the grain boundary.

Fig. 12 shows the microstructure of diagonal section after compression along ND direction. It can be seen that the crack started from the compression face and developed along the grain boundary and ended at the three crystal cross position.

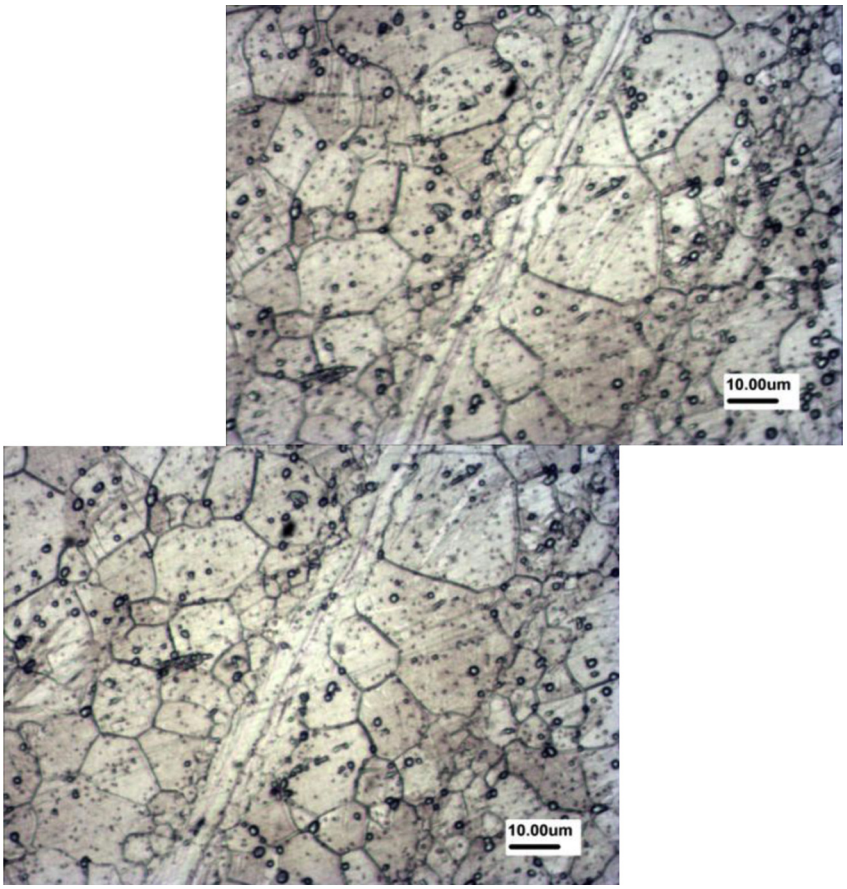

Fig. 9. Microstructure of the diagonal section after compression along the TD direction under strain rate of 2552 s^{-1}.

4. Discussion

4.1. Deformation localization

The results above manifest that the deformation localization of extruded Mg-Gd-Y magnesium alloy after dynamic compression can be seen in three aspects: pullulation and growing up of crystallized grains, forming of twins in several grains and forming of white shear band.

4.1.1. Pullulation and growing up of recrystallized grains

Ion [13] thought that, the reasons that magnesium alloys can be easily dynamically recrystallized are: (1) there are fewer slip systems of magnesium alloys and piling up of dislocations happens easily so that dislocation density can meet the standard for dynamic recrystallization; (2) magnesium and its alloys have lower stacking fault energy and extended dislocation is hard to strand, so it is difficult to slip and climb and dynamically recover slowly but improve recrystallization; (3) magnesium alloys have higher speed of the grain boundary diffusion and the dislocation energy piled up on the subgrain boundaries can be absorbed by the boundaries which can speed up the dynamic recrystallization. The grains of dynamic recrystallization are relevant not only to the size of deformation degree, but also to the temperature of deformation and strain rate. The higher the temperature is, the more sufficient dynamic recrystallization is and the more homogeneous microstructure is. But grain boundary diffusion and grain boundary migration are improved and grains grow up easily which leads to coarse grain. While with strain rate being increased, the time is too short for dislocations generated in the deformation. It leads to grain refinement that dislocations increase and crystallization nuclei increases. Dynamic recrystallization grains generally coarsening at the grain boundary or near the grain boundary. Because deformation continues during the nucleation and growth of recrystallized grains, a certain degree of strain exists in the dynamic recrystallization grains which are quite different from the equiaxed grains without distortion after recrystallization annealing [14]. In original microstructure of extruded Mg-Gd-Y magnesium alloy, there are a great amount of uniform equiaxed big-sized grains and a small amount of small sized recrystallization grains. Different sized grains are the microstructure foundation of the inhomogeneity under high speed deformation. With the strain rates increased, recrystallization grains absorb the impact energy and populate and grow up so that the uncontinuous recrystallization bands become continuous and wide.

4.1.2. Forming of twins in several grains

There are no twins in the original microstructure of extruded Mg-Gd-Y magnesium alloy, but the amount of twins increases and then decreases with strain rates being increased. Under the strain rate of about 1500 s^{-1} (ED direction:1392 s^{-1}, TD

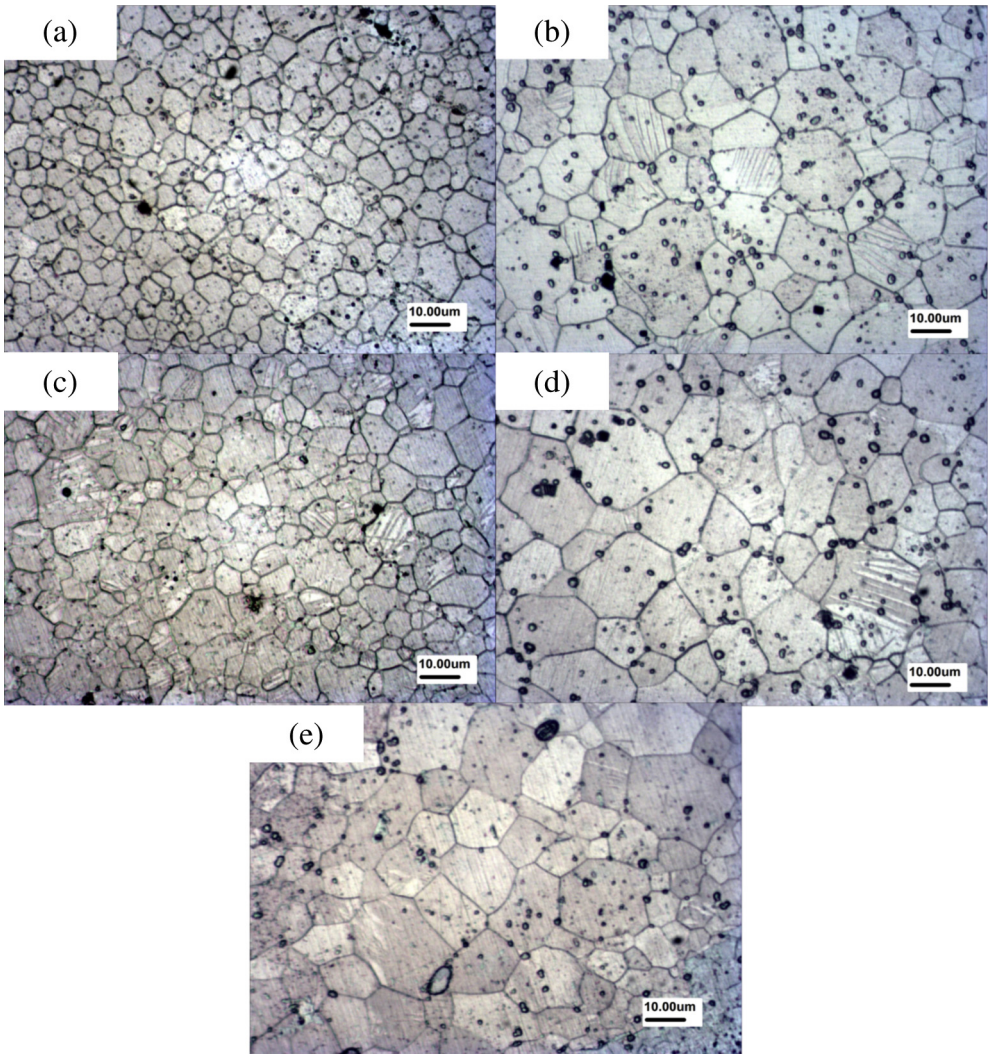

Fig. 10. Microstructures of section perpendicular to loading direction along ND direction: (a) original microstructure; (b) under strain rate of 1101 s^{-1}; (c) under strain rate of 1488 s^{-1}; (d) under strain rate of 1911 s^{-1}; (e) under strain rate of 2529 s^{-1}.

direction:1508 s^{-1}, ED direction:1488 s^{-1}),the amount of the twins is the maximum. It implies that the microstructure of extruded Mg-Gd-Y magnesium alloy is sensitive to strain rates, which is similar to the phenomenon observed in the microstructure of AZ31B magnesium alloy after dynamic compression [15]. In addition, it indicates that under the lower strain rates, the dynamic compressive deformation mechanism of extruded Mg-Gd-Y magnesium alloy is twinning; while under the higher strain rates, the dynamic compressive deformation mechanisms of extruded Mg-Gd-Y magnesium alloy are twinning and slip. The higher strain rate is, the more percentage of slip is. This is because magnesium alloys have less slip systems at room temperature and it causes a strong stress concentration near the grain boundaries. The strong stress concentration can improve the formation of twins and coordinate the plastic deformation. When strain rates and temperatures increase, cross slip and non-basal slip can start although the critical shear stress decreases which twinning needs. The amount of starting slip is increased so that the stress concentration has weakened and it is against the formation of twins. As a result, twinning makes a less contribution to the plastic deformation at high strain rates. On the contrary non-basal slip which has thermal activation characteristics can play an important role during the release of stress concentration and the coordination of plastic deformation. In addition, during the plastic deformation twinning will choose to appear in advantageously oriented grains. It explains that twinning happens in only several grains which are not only big-sized grains but also small sized grains whose orientations are advantaged.

4.1.3. Forming of white shear band

Unlike the quasi-static deformation, during the dynamic deformation under high speed impact loading, materials step into the macroscopic plastic instability stage after certain plastic deformation and shear deformation localization occurs on the microscopic level. Because deformation heat is difficulty to be released in a very short time, shear deformation occurs under a nearly adiabatic circumstance. The major character of this failure mechanism is a large amount of deformation and high temperature rising in a narrow deformation band which can be observed and be named as an

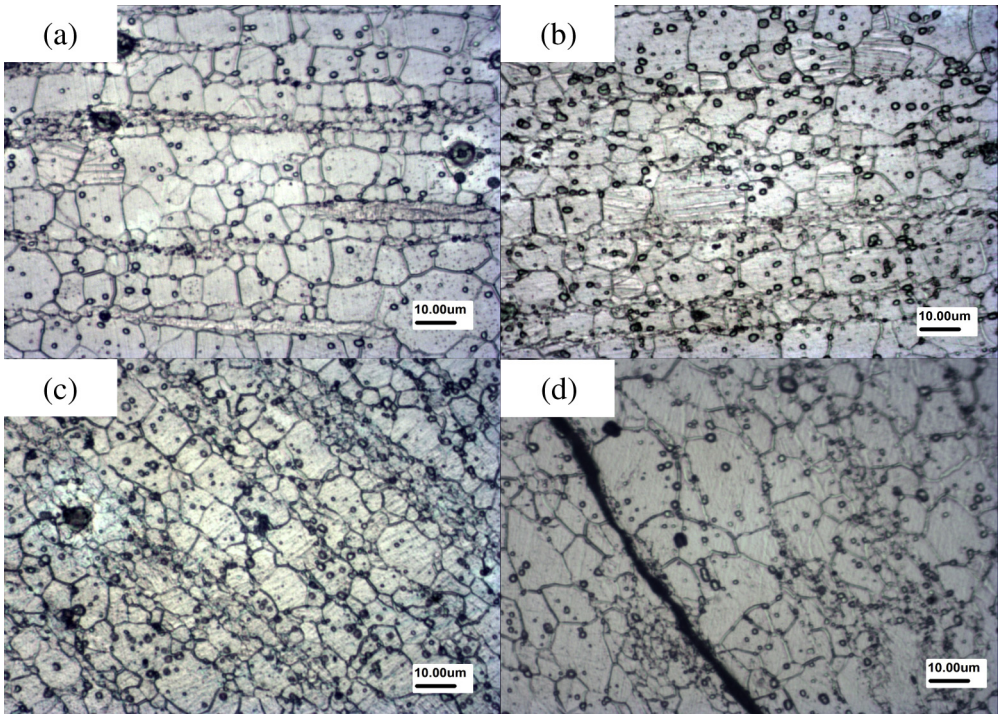

Fig. 11. Microstructures of section parallel with loading direction along ND direction: (a) under strain rate of 1101 s^{-1}; (b) under strain rate of 1488 s^{-1}; (c) under strain rate of 1911 s^{-1}; (d) under strain rate of 2529 s^{-1}.

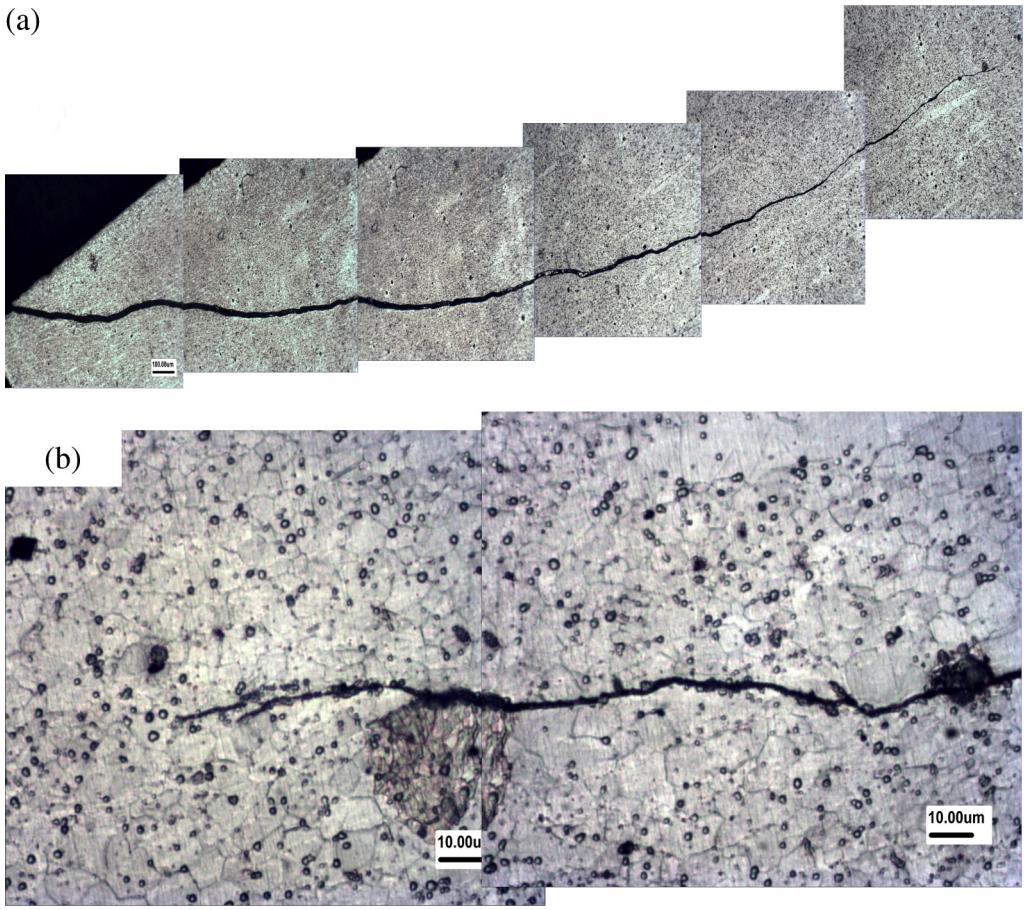

Fig. 12. Microstructure of diagonal section after compression along ND direction under strain rate of 2529 s^{-1}: (a) 100×; (b) 800×.

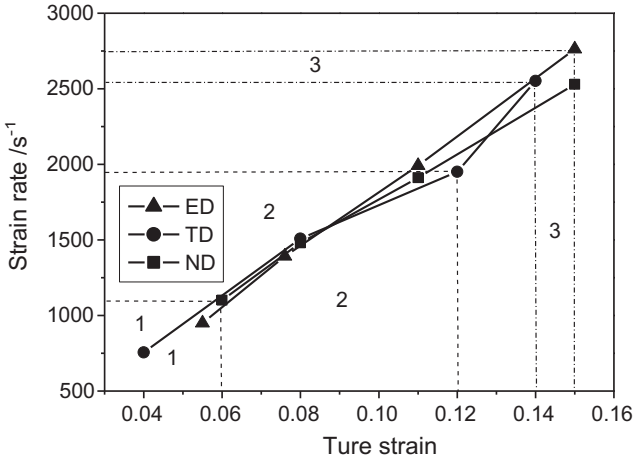

Fig. 13. Dynamic compressive strain rates-true strain curves of Mg-Gd-Y magnesium alloy.

adiabatic shear band (ASB). Because ASB points out the essential difference between the mechanisms of dynamic deformation and quasi-static deformation, scientists around the world have done so many researche works on ASB from the theoretical and the experimental aspect [16–18]. The reason why ASB is called "white band" is that no matter using ordinary light or using secondary electron this kind of substructure shows "white" [19]. Ji Wei and Fan Ya-fu [9] found that Mg-Gd-Y alloys can form two kinds of ASB respectively by ballistic impact test and SHPB test at high temperature. ASB formed during ballistic impact shows white under optical microscope and its average width is 10 μm. The microhardness in the ASB is higher than that around the matrix. But in SHPB test at high temperature, obvious plastic deformation bands are observed only when $T = 735$ K. The analysis of microstructure in the present experiment proves that, Mg-Gd-Y magnesium alloys can form ASB in SHPB test at room temperature. Fig. 13 shows the dynamic compressive strain rates-true strain curves of Mg-Gd-Y magnesium alloy. Zone 1 shows the beginning of the deformation and there is no ASB. When the strain rates are from 1000 s^{-1} to 2000 s^{-1} and strains are from 0.08 to 0.12 (as shown in Fig. 13 zone 2), extruded Mg-Gd-Y magnesium alloys can all form uncontinuous white ASB along ED, TD and ND directions. When the strain rate is above 2500 s^{-1} and the strains are from 0.14 to 0.15 (as shown in Fig. 13 zone 3), continuous white ASB appear only in section parallel with loading direction along ED and in section perpendicular to the loading direction along TD but there is no continuous white ASB along ND. It indicates that the forming of ASB of extruded Mg-Gd-Y magnesium alloys is relative not only to the strain rate and strain but also to the orientation of crystal grains and texture.

Magnesium alloys form strong (0002) basal texture easily during the plastic deformation of extruding and rolling [20]. Fig. 14 is the texture pole figure of extruded Mg-Gd-Y magnesium alloy. There is strong (0002) basal texture along ED. The basal planes of most grains are parallel to ED and the $(10\bar{1}0)$ prismatic planes of small amounts of grains are parallel to ED. Under the strain rates from 1000 s^{-1} to 2000 s^{-1}, a large numbers of twins formed and they have the effect on adjusting orientation of grains and releasing stress concentration and stimulating further slip [21]. That is to say, the twins play an important role of forming ASB either.

Through the above analysis we can conclude that, the formation process of the adiabatic shear band can be divided into three stages. In the first stage, under the impact loads a great deal of twins formed and the deformation mechanism is twinning. In the second stage, discontinuous ASB forms and the deformation mechanisms are twinning and non-basal slip. In the last stage, non-basal slip turns to basal slip and continuous ASB forms.

4.2. Deformation isothermal

Deformation isothermal is reflected in the process of the forming of ASB and the abnormal big grain (shown in Fig. 8(c) and (d)). This is because under high strain rates, the whole deformation is in a very short time and a large part

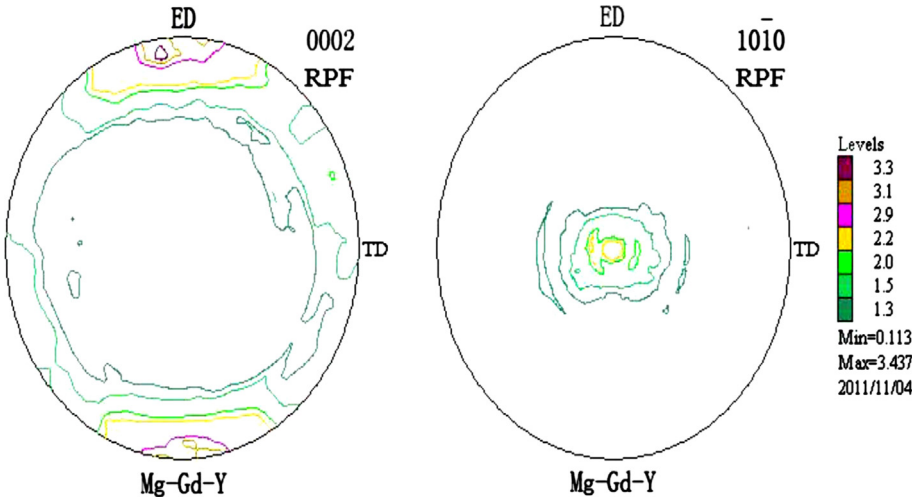

Fig. 14. (0002) Pole figure of extruded Mg-Gd-Y magnesium alloy.

(about 90%) of plastic work turns into heat and the time is too short for heat to release. Heat concentration leads several grains growing up abnormally by grain boundary migration to absorb adjacent grains. Adiabatic temperature rising causes the effect of thermal softening [22]. When this effect becomes a major effect, the ASB will form.

4.3. Failure mechanisms

Based on the microstructures, the dynamic compression fracture mechanism of extruded Mg-Gd-Y Magnesium alloy is multi-crack propagation (as shown in Fig. 6). The crack started from the compression surface and developed along the grain boundary and ended at the three crystal cross position (as shown in Fig. 12). It can also explain why thin-walled square cylindrical specimen made of magnesium alloy falls into small fragments after plastic instability in the impact test, which simulating auto crashing, while thin-walled square cylindrical specimen made of steel or aluminum alloy performs plastic folds to absorb impact energy [23]. So it is inaccurate to use the existing mechanisms of ASB and failure mechanisms of steel, aluminum alloy, titanium and its alloy to investigate magnesium alloy. It requires more researches on the dynamic fracture mechanism of magnesium alloy, especially on the relationship between ASB and crack initiation.

5. Conclusions

(1) Microstructures of extruded Mg-Gd-Y Magnesium alloy along ED, TD and ND compression directions are sensitive to strain rates. The amount of twins firstly increases and then decreases with strain rates being increased. The twins play an important role of farming.
(2) With increased strain rates, the crystal grains increase and grow up.
(3) The formation process of the adiabatic shear band can be divided into three stages. In the first stage, under the impact loads a great deal of twins form and the deformation mechanism is twinning. In the second stage, discontinuous ASB forms due to twins adjusting the directions of located grains and the deformation mechanisms are twinning and non-basal slip. In the last stage, non-basal slip turns to basal slip and continuous ASB forms.
(4) The dynamic compression fracture mechanism of extruded Mg-Gd-Y Magnesium alloy is multi-crack propagation.

Acknowledgments

The authors would like to acknowledge the financial support from the Ministry of Science and Technology of People's Republic of China (National Basic Research Program of China, No: 2011BAE22B05, Research and evaluation of magnesium alloy protection, connectivity and reliability) and a Science and Technology Plan of Liaoning Province, China, No: 201202160, Research of the mechanism of ASB in AZ31 Magnesium alloy under high speed impact.

References

[1] L.I.U. Zheng, W.A.N.G. Yue, W.A.N.G. Zhong-guang, L.I. Feng, S.H.E.N. Zhi-yong, Chinese Journal of Material Research 14 (5) (2000) 449−456.
[2] C.H.E.N. Li-he, Z.H.A.O. Hui-jie, L.I.U. Zheng, S.H.E.N. Zhi-yong, N.I.E. Yi-yong, Foundry 10 (1999) 45−50.
[3] S.H.E.N. Yuan-xiang, Z.H.A.N.G. Xiu-rong, L.U.O. Ming-wen, Journal of Sichuan Ordnance 29 (5) (2008) 114−116.
[4] W.U. Yu-juan, D.I.N.G. Wen-jiang, P.E.N.G. Li-ming, Z.E.N.G. Xiao-qin, L.I.N. Dong-liang, Materials China 30 (2) (2011) 1−9.
[5] J.I. Wei, F.A.N. Ya-fu, C.H.E.N. Jie, W.A.N.G. Jun, Journal of Materials Engineering 10 (2009) 41−44.
[6] M.A.O. Ping-li, L.I.U. Zheng, W.A.N.G. Chang-yi, W.A.N.G. Feng, Materials Review 26 (4) (2012) 95−101.
[7] Zong-yong Yao. Quantitative investigation of microstructural and texture evolution during cold rolling Aa3104 and Aa1050 aluminum alloys, Doctoral Dissertation. Beijing: Tsinghua University, Department of Materials, 2009.
[8] Y.I.N. Jia-ming, L.I. Bo-long, H.A.N. Peng, Z.H.A.N.G. Qing-hua, L.I.U. Tong, N.I. Zuo-ren, Science Technology and Engineering 12 (17) (2012) 4119−4123.
[9] J.I. Wei, F.A.N. Ya-fu, C.H.E.N. Jie, Q.I.A.O. Guang-li, Rare Metal Materials and Engineering 38 (4) (2009) 599−602.
[10] S.W. PARK, M. ZHOU, Experimental Mechanics 39 (4) (1999) 287−294.
[11] S.O.N.G. Li, H.U. Shi-sheng, Explosion and Shock Waves 25 (4) (2005) 368−373.
[12] S.O.N.G. Bo, S.O.N.G. Li, H.U. Shi-sheng, Explosion and Shock Waves 18 (2) (1998) 167−171.
[13] S.E. Ion, F.J. Humphreys, S.H. White, Acta Metallurgica 30 (1982) 1909−1919.
[14] C.H.E.N. Zhen-hua, X.U. Fang-yan, F.U. Ding-fa, X.I.A. Wei-jun, Chemical Industry and Engineering Progress 25 (2) (2006) 140−146.
[15] M.A.O. Ping-li, L.I.U. Zheng, W.A.N.G. Chang-yi, J.I.N.G. Xin, W.A.N.G. Feng, G.U.O. Quan-ying, et al., The Chinese Journal of Nonferrous Metals 19 (5) (2009) 817−820.
[16] H.C. Rogers, Annual Review of Materials Science 9 (1979) 283−311.
[17] Y.L. Bai, B. Dodd, Pergamon Press, Oxford, UK, 1992. pp. 24−53.
[18] T.W. Wright, Cambridge University Press, Cambridge, UK, 2002. pp. 1−32.
[19] Y.B. Xu, Y.L. Bai, M.A. Meyers, Journal of Materials Science &Technology 22 (2006) 737−746.
[20] C.H.E.N. Zhen-hua, X.I.A. Wei-jun, C.H.E.N. Yong-qi, F.U. Ding-fa, The Chinese Journal of Nonferrous Metals 15 (1) (2005) 1−11.
[21] X.I.A.O. Yang, Z.H.A.N.G. Xin-ming, Special Casting & Nonferrous Alloys 30 (10) (2010) 958−961.
[22] Y.A.N.G. Yang, C.H.E.N.G. Xin-lin, The Chinese Journal of Nonferrous Metals 12 (3) (2002) 402−407.
[23] Zheng Liu, Pingli Mao. A Canada-China- USA collaborative research and development project: magnesium front end research and development 2008 annual progress report,14−32; 2008.